Journal of Peptide Science
J. Peptide Sci. **5**: 161–175 (1999)

Conformational Analyses of Cyclic Hexapeptide Analogs of Somatostatin Containing Arylalkyl Peptoid and Naphthylalanine Residues

RALPH-HEIKO MATTERN, THUY-ANH TRAN and MURRAY GOODMAN*

Department of Chemistry and Biochemistry, University of California at San Diego, La Jolla, CA 92093-0343, USA

Received 2 May 1998
Accepted 28 July 1998

Abstract: We report the conformational analysis by ^{1}H-NMR in DMSO and computer simulations involving distance geometry and molecular dynamics simulations of peptoid analogs of the cyclic hexapeptide *c*-[Phe^{11}-Pro^{6}-Phe^{7}-D-Trp^{8}-Lys^{9}-Thr^{10}] L-363,301 (the numbering refers to the positions in native somatostatin). The compounds *c*-[Phe^{11}-Nphe^{6}-Nal^{7}-D-Trp^{8}-Lys^{9}-Thr^{10}] (**Nphe^{6}-Nal^{7}** analog **1**), *c*-[Nal^{11}-Nphe^{6}-Phe^{7}-D-Trp^{8}-Lys^{9}-Thr^{10}] (**Nal^{11}-Nphe^{6}** analog **2**) and *c*-[Phe^{11}-Nnal^{6}-Phe^{7}-D-Trp^{8}-Lys^{9}-Thr^{10}] (**Nnal^{6}** analog **3**), where Nphe denotes *N*-benzylglycine and Nnal denotes *N*-(1-naphthylmethyl)glycine, are subjected to SAR studies in order to investigate the influence of the bulky naphthyl aromatic ring on the conformation. The **Nal^{11}-Nphe^{6}** and **Nphe^{6}-Nal^{7}** analogs exhibit potent binding to the hsst2, hsst3 and hsst5 receptors, whereas the **Nnal^{6}** analog has decreased binding affinity to all receptors but is more selective towards the hsst2 than the other two analogs and L-363,301. The conformational search employing distance geometry, energy minimization and molecular dynamic simulations gives insight into the conformational flexibility of these analogs. The molecules adopt both *cis* and *trans* orientations of the peptide bond between residues 11 and 6. The *cis* isomers of these analogs adopt type II′ β-turns with D-Trp in the $i+1$ position and type VI*a* β-turns with the *cis* peptide bond between residues 6 and 11. The results of free and distance restrained molecular dynamics simulations at 300 K indicate that the **Nphe^{6}-Nal^{7}** and **Nal^{11}-Nphe^{6}** compounds adopt a preferred backbone conformation which can be described as ‘folded’ about residues 7 and 10. The **Nnal^{6}** analog, which binds less effectively to the hsst receptors, has a more flexible backbone structure than the **Nal^{11}-Nphe^{6}** and **Nphe^{6}-Nal^{7}** analogs and prefers a ‘flat’ structure with regard to the orientations about Phe^{7} and Thr^{10} during molecular dynamics simulations. Copyright © 1999 European Peptide Society and John Wiley & Sons, Ltd.

Keywords: conformational analysis; somatostatin analogs; peptoids; ^{1}H-NMR; computer simulations

INTRODUCTION

Somatostatin, a heterodetic cyclic tetradecapeptide, inhibits the release of several hormones (e.g. glucagon, growth hormone, insulin, gastrin) [1–3]. Veber *et al.* carried out extensive structure-activity relationship studies, which led to the synthesis of the highly potent somatostatin analog L-363,301, *c*-[Phe^{11}-Pro^{6}-Phe^{7}-D-Trp^{8}-Lys^{9}-Thr^{10}] [4] (the numbering refers to the location of the residues in native somatostatin). The discovery of this cyclic hexapeptide, which in certain assays is more potent than native somatostatin, initiated the synthesis of numerous cyclic hexapeptides related to somatostatin. Studies of their conformations in solution [5–10] revealed that L-363,301 and most of the related active compounds share common structural motifs

Abbreviations: DG, distance geometry; DMSO-d_6, fully deuterated dimethyl sulfoxide; DQF-COSY, double-quantum filtered correlation spectroscopy; Nal, 1-naphthylalanine; Nnal, *N*-(1-naphthylmethyl)glycine; ROESY, rotating frame nuclear Overhauser enhancement spectroscopy; TOCSY, total correlation spectroscopy.

* Correspondence to: Department of Chemistry and Biochemistry, University of California at San Diego, La Jolla, CA 92093-0343, USA. E-mail: mgoodman@ucsd.edu

CCC 1075–2617/99/040161-15$17.50

such as a type II′ β-turn with D-Trp in the $i+1$ position and a type VI*a* β-turn in the so-called bridging region Xaa^{11}-Xbb^{6} characterized by a *cis* peptide bond or mimicked by a disulfide or lanthionine bridge as in sandostatin analogs [11,12].

From these investigations it has been deduced that the tetrapeptide sequence Phe^{7}-D-Trp^{8}-Lys^{9}-Thr^{10} is the biologically active portion, interacting with the receptor, while the Xaa^{11}-Xbb^{6} sequence is important for maintaining the proper orientation of the tetrapeptide sequence and contains a hydrophobic portion interacting with the receptors. Conformational studies on L-363,301 have also shown that the molecule adopts two backbone conformations which are both consistent with all NMR data: a 'flat' conformation and a structure which is 'folded' about Phe^{7} and Thr^{10} [13]. Both structures contain a type II′ β-turn spanning D-Trp and Lys as well as a type VI*a* β-turn in the bridging region 11–6. The 'folded' structure contains two additional γ-turns about residues 10 and 7.

The conformational analysis of a series of α- and β-methylated analogs of L-363,301 revealed valuable information regarding the 'bioactive' conformation of the side chains and of the backbone by restricting the conformational flexibility of these analogs compared with the parent compound [14,15]. These studies suggested that the 'folded' and not the 'flat' conformation might be the 'bioactive' structure and revealed a side chain topology for active somatostatin analogs. In particular, the D-Trp side chain adopts preferably a *trans* orientation in the 'bioactive' conformation, whereas the Lys side chain adopts a g^{-} orientation. This arrangement results in a close spatial proximity of the side chains of D-Trp and Lys. This proximity has earlier been postulated based upon the upfield shift of the Lys γ-protons in the ^{1}H-NMR. This upfield shift was explained by shielding of the Lys γ-protons caused by the aromatic side chain of D-Trp [16].

We have recently reported SAR studies of a series of analogs of L-363,301 in which the Pro residue in position 6 was replaced with the peptoid residues N-benzylglycine (**Nphe^{6}** analog), and (S) or (R)-α-methylbenzylglycine (**(S)** or **(R)-β-MeNphe^{6}** analogs) [17–19]. These compounds are selective towards the hsst2 receptor compared with L-363,301 and selectively inhibit *in vivo* the release of growth hormone while they have no effect on the release of insulin.

This paper reports on the conformational analysis of the cyclic hexapeptide somatostatin analogs *c*-[Phe^{11}-$Nphe^{6}$-Nal^{7}-D-Trp^{8}-Lys^{9}-Thr^{10}] (**Nphe^{6}-Nal^{7}** analog, **1**), *c*-[Nal^{11}-$Nphe^{6}$-Phe^{7}-D-Trp^{8}-Lys^{9}-Thr^{10}] (**Nal^{11}-Nphe^{6}** analog, **2**), and *c*-[Phe^{11}-$Nnal^{6}$-Phe^{7}-D-Trp^{8}-Lys^{9}-$Thri^{10}$] (**Nnal^{6}** analog, **3**) which were studied by ^{1}H-NMR in DMSO-d_6 and by computer simulations. We envisioned that the incorporation of the larger Nnal peptoid residue in position 6 or the introduction of Nal residues in either position 7 or 11 would lead to conformationally more restricted analogs compared with the parent compound *c*-[Phe^{11}-$Nphe^{6}$-Phe^{7}-D-Trp^{8}-Lys^{9}-Thr^{10}] (**Nphe^{6}** analog). The **Nal^{11}-Nphe^{6}** analog **2** shows similar binding affinities to the hsst2, 3 and 5 receptors as compound L-363,301. The **Nphe^{6}-Nal^{7}** analog is more selective to the hsst2 and exhibits very similar hsst5/hsst2 and hsst3/hsst2 ratios as the **Nphe^{6}** analog. The **Nnal^{6}** compound **3** exhibits reduced binding affinities to all hsst receptors compared with L-363,301 and compared with the other two analogs but it has the highest selectivity towards the hsst2 receptor. A detailed discussion of the bioactivity data and the synthesis is given in the accompanying paper [20].

MATERIALS AND METHODS

^{1}H-NMR Measurements

The ^{1}H-NMR spectra were recorded on a Bruker AMX 500 spectrometer operating at 500 MHz. Temperatures were maintained at given values within ± 0.1°C. All experiments were carried out in DMSO-d_6 with the solvent peak ($=2.49$ ppm) as internal standard. The peak assignments were made using TOCSY [21–23], DQF-COSY [23–26] and the ROESY [27] experiments. The TOCSY experiments employed the MLEV-17 spin locking sequence suggested by Bax and Davis [21] with a spin locking field of 10 kHz. A mixing time of 75 ms was used. The ROESY experiments were carried out using mixing times of 100 and 200 ms with a spin locking field of 2.5 kHz. All two-dimensional spectra were obtained using 4K data points in the $f2$ domain and 400 points in the $f1$ domain for the TOCSY and ROESY experiment and 512 data points in the $f1$ domain for the DQF-COSY. The time proportional phase increment was used. Applying zero filling procedures resulted in a final matrix of $2K \times 2K$ data points. Multiplication with a 30° shifted sine bell function was used for the TOCSY and DQF-COSY and multiplication with a 90° shifted sine bell function was applied for the ROESY to enhance the spectra. The ROESY crosspeaks were calibrated against the distance between the indole HN and H2 protons of D-Trp^8 and against the geminal protons of the peptoid residue where possible. The ROESY experiment was used for the sequential assignments [28]. The ROEs observed in the ROESY experiment were assigned as strong, medium and weak relative to each other according to their intensities. An error of ± 0.5 Å was estimated and the upper and lower distances were set to the measured distance of ± 0.5 Å. The $J_{NHC^{\alpha}H}$ coupling constants were used to calculate the ϕ angles [29,30]. The $J_{C^{\alpha}H\text{-}C^{\beta}H}$ coupling constants were used to calculate the side chain populations. For the calculation of aliphatic amino acids, Pachler's equations [31] were used, while Cung's equations [32] were used for aromatic residues. The stereospecific assignments necessary for the calculations were carried out as described by Yamazaki *et al.* [33].

Computer Simulation

All calculations were performed on an Iris 4D-340 computer (Silicon Graphics). The distance geometry program DGEOM [34] was used to generate structures consistent with the distance constraints derived from the NOEs. Temperature coefficient of NH protons indicating hydrogen bonds and ϕ angles calculated from $J_{NH\text{-}H^{\alpha}}$ were used to filter out structures that did not meet the experimental data. An error of $\pm 30°$ was tolerated for the ϕ angles calculated from $J_{NH\text{-}H^{\alpha}}$ at this stage of refinement. In the case of the hydrogen bond based selection, structures were retained in which the NH protons with an absolute value of the temperature coefficient < 2 ppb/K donate at least one hydrogen bond fulfilling the loose threshold of 3.0 Å and 110° for the NH proton-acceptor distance and for the angle defined by the three atoms N-H-O of the acceptor carbonyl. Structures which did not fulfill these requirements were discarded. The remaining structures were subjected to molecular dynamics. Energy minimization and molecular dynamics computation were carried out *in vacuo* using the DISCOVER program [35] with the CFF91 force field. To approximate the solvation, a distance-dependent dielectric constant was used. In order to search the accessible space more thoroughly, the distance geometry structures which were consistent with the experimental data, were subjected to 10 ps of molecular dynamics at 1000 K with a step size of 1 fs. At intervals of 1 ps, conformations were extracted and energy minimized by steepest descent until the maximum derivative was less than 1. Starting from each of the minimized structures 10 ps of molecular dynamics was performed at 300 K. At regular intervals of 1 ps structures were extracted. These structures were subjected to unrestrained minimization using the VA09A algorithm until the maximum derivative was less than 0.001 kcal/mol. Using this procedure, 100 structures were created starting from each of the remaining distance geometry structures. The structures which were consistent with the temperature coefficients, calculated ϕ angles and NOEs derived from the ROESY experiment were subjected to cluster analysis using a range of $\pm 30°$ of the backbone torsional angles. Deviations less than 20° were tolerated for the ϕ angles estimated from the $J_{NH\text{-}H^{\alpha}}$ at this stage of the refinement. The other conformations were discarded. The low energy conformation of each conformational family was subjected to free molecular dynamics at 300 K.

RESULTS

NMR Studies

The relevant NMR data are presented in Tables 1–4.

Two sets of spin systems were observed in the ^{1}H-NMR spectra of the three analogs corresponding to *cis* and *trans* orientation of the peptide bond between residues 11 and the peptoid residues. The *cis* isomer is in all three compounds higher populated and the ratios of *cis*:*trans* as determined by integration are 1.6:1 for the **Nphe^6-Nal^7** compound **1**, 1.4:1 for the **Nal^{11}-Nphe^6** compound **2**, and 3.5:1 for the **Nnal^6** compound **3**.

The experimental proof for the *cis* peptide bond between residues 11 and 6 is a strong NOE between the two CH$^{\alpha}$ protons of residues 11 and 6. The less populated conformation shows a strong NOE between the Xaa^{11}H$^{\alpha}$ and the β-protons of the peptoid residue, which supports a *trans* orientation of the peptide bond. The observation of several exchange crosspeaks between the *cis* and *trans* conformation in the ROESY spectrum ($\tau_{mix} = 200$ ms) of the **Nphe^6-Nal^7** analog **1** indicates that the *cis–trans* isomerization occurs relatively fast on this time scale. Contrary to that, the **Nal^{11}-Nphe^6** analog **2** and the **Nnal^6** analog **3** do not show exchange cross peaks, suggesting that the *cis–trans* isomerization in these compounds occurs more slowly than in the **Nphe^6-Nal^7** analog **1**. This can be explained by the fact that the bulky Nal or Nnal residue in the **Nal^{11}-Nphe^6** analog **2** and the **Nnal^6** analog **3** is positioned within the residue 11 or 6 which are directly involved in the *cis–trans* isomerization.

Table 1 Backbone NOEs from ROESY Experiment of *c*-[Phe^{11}-Nphe^{6}-Nal^{7}-D-Trp^{8}-Lys^{9}-Thr^{10}] (**1**), *c*-[Na^{11}-Nphe^{6}-Phe^{7}-D-Trp^{8}-Lys^{9}Thr^{10}] (**2**) and *c*-[Ph^{11}-Nnal^{6}-Phe^{7}-D-Trp^{8}-Lys^{9}-Thr^{10}] (**3**)

	Phe^{11}-Nphe^{6}-Nal^{7}		Nal^{11}-Nphe^{6}-Phe^{7}		Phe^{11}-Nnal-Phe^{7}	
	cis	*trans*	*cis*	*trans*	*cis*	*trans*
Xa^{11}NH-Xaa^{11}H$^{\alpha}$	m (2.7)	m (2.7)	m (2.6)	m (2.6)	m (2.8)	m (2.6)
Xa^{11}NH-ThrH$^{\alpha}$	s (2.3)	s (2.2)	s (2.3)	s (2.4)	s (2.4)	s (2.5)
Xaa^{11}H$^{\alpha}$-Xaa^{6}H$^{\alpha}$	s (1.8)	–	s (1.8)	–	s (1.9)	–
Xa^{11}H$^{\alpha}$-Xaa^{6}H$^{\alpha}$	–	s (2.0)	–	s (2.0)	–	s (2.1)
Xaa^{7}NH-Xaa^{7}H$^{\alpha}$	m (2.7)	m (2.4)	m (2.6)	m (2.5)	m (2.7)	s (2.5)
Xaa^{7}NH-Xaa^{6}H$^{\alpha}$	overlap	w	m (3.0)	m (2.5)	m (2.9)	s (2.4)
TrpNH-Xaa^{7}H$^{\alpha}$	s (2.1)	s (2.2)	s (2.1)	s (2.0)	m (3.0)	s (2.3)
TrpNH-TrpH$^{\alpha}$	m (2.8)	m (2.7)	m (2.7)	m (2.7)	m (2.8)	m (2.8)
LysNH-LysH$^{\alpha}$	m (2.9)	m (2.9)	m (2.8)	m (2.7)	m (2.8)	m (3.0)
LysNH-TrpH$^{\alpha}$	s (2.1)	s (2.1)	s (2.0)	s (2.0)	s (2.1)	s (2.1)
ThrNH-ThrH$^{\alpha}$	m (3.3)	m (2.8)	m (3.2)	m (2.7)	m (overlap)	m (2.7)
ThrNH-LysH$^{\alpha}$	m (2.9)	m (2.9)	overlap	m (3.0)	m (3.0)	m (2.9)
LysNH-ThrNH	m (2.6)	m (2.7)	m (2.5)	m (2.5)	s (2.5)	m(2.6)
TrpNH-Xaa^{7}NH	m (3.3)	–	m (3.4)	–	m (3.0)	m (3.1)
TrpNH-ThrNH	–	–	–	–	m (3.3)	–
Xaa^{11}NH-ThrNH	w (3.8)	–	w (4.0)	–	m (3.2)	–
Xaa^{7}NH-Xa^{11}H$^{\alpha}$	m (3.0)	–	m (2.8)	–	m (2.9)	–

[a] The NOEs corresponding to distances ≤2.5 Å are classified as strong (s); corresponding to distances >2.5 Å and <3.5 Å are classified as medium (m); the NOEs corresponding to distances >3.5 Å and ≤4.5 Å are classified as weak (w).

Medium NOEs between the NH protons of Thr^{10} and Lys^{9} and the absence of NOEs between the NH protons of Lys^{9} and D-Trp^{8} suggest a type II′ β-turn with D-Trp^{8} in the $i+1$ position for the *cis* isomers of all three compounds. This is consistent with the low temperature coefficients of the Thr^{10}NH protons and with strong sequential NOEs between Lys^{9}NH and D-Trp^{8}H$^{\alpha}$, medium NOEs between Thr^{10}NH and Lys^{9}H$^{\alpha}$ and medium NOEs between Lys^{9}NH and Lys^{9}H$^{\alpha}$. In the **Nnal^{6}** compound **3** a medium NOE between D-Trp^{8}HN and Thr^{10}HN is observable which is not consistent with a type II′ β-turn. This NOE is not present in the ROESY spectra of the **Nphe^{6}-Nal^{7}** analog **1** and the **Nal^{11}-Nphe^{6}** analog **2**.

Besides the ThrNH there are no NH protons with temperature coefficients low enough to indicate involvement in hydrogen bonds. This implies that the hydrogen bond within the type VI β-turn formed by the *cis* peptide bond is not very rigid. The type VI β-turn is indicated by NOEs between Phe^{7}NH and the Ph^{11}H$^{\alpha}$.

In the *cis* isomers of all three compounds, there are two other NOEs observable between NH protons of different residues, medium NOEs between D-Trp^{8}NH and Nal^{7}NH and weak to medium NOEs between Phe^{11}NH and Thr^{10}NH. These NOEs were not observable in the **Nphe^{6}** analog [19] and indicate a higher population of the 'folded' backbone conformation in the Nal or Nnal containing analogs compared with the **Nphe^{6}** analog.

For the **Nphe^{6}-Nal^{7}** analog **1**, the Nal in position 7 leads to a close proximity between the D-Trp and Lys side chains. This is proven by the presence of several NOEs, such as a medium NOE between the D-Trp aromatic proton H2 and the Lys γ protons, a weak NOE between the D-Trp aromatic NH and Lys ε protons and a weak NOE between the D-Trp aromatic NH and the Lys δ protons. Proximity between the Nal side chain and the Trp residue in the **Nphe^{6}-Nal^{7}** analog **1** is suggested by the presence of a weak NOE between the H^{7} proton of the Nal aromatic ring and D-TrpH$^{\alpha}$. No such NOEs were observed for the Nal^{11} **Nphe^{6}** analog **2** and the **Nnal^{6}** compound **3**.

The *trans* isomers of the compounds **1**–**3** have two NH protons with low temperature coefficients, the Xaa^{7}NH and the Thr^{10}NH (**Nphe^{6}-Nal^{7}** analog **1** and the **Nnal^{6}** compound **3**) or the Na^{11}HN (**Nal^{11}-Nphe^{6}** analog **2**). Medium NOEs between the Thr^{10}NH and the Lys^{9}NH protons indicate turns

Table 2 $J_{\text{H-N-H}^{\alpha}}$ Coupling Constants (in Hz) and Calculated ϕ Angles of *c*-[Phe^{11}-Nphe^{6}-Nal^{7}-D-Trp^{8}-Lys^{9}-Thr^{10}] (**1**), *c*-[Nal^{11}-Nphe^{6}-Phe^{7}-D-Trp^{8}-Lys^{9}-Thr^{10}] (**2**), *c*-[Phe^{11}-Nal^{6}-Phe^{7}-D-Trp^{8}-Lys^{9}-Thr^{10}] (**3**)

	Phe^{11}-Nphe^{6}-Nal^{7}		Nal^{11}-Nphe^{6}-Phe^{7}		Phe^{11}-Nnal^{6}-Phe^{7}	
	cis	*trans*	*cis*	*trans*	*cis*	*trans*
Xaa^{11}	4.7 Hz	6.2 Hz	5.2 Hz	3.3 Hz	4.5 Hz	<2 Hz
	100	88	96	110	101	
	20	32	24	10	19	
	−169	−160	−166	−178	−170	
	−71	−80	−74	−61	−70	
Nal^{7}	6.3 Hz	9.1 Hz	6.5 Hz	6.3 Hz	6.5 Hz	7.6 Hz
	87	−138	85	87	86	73
	33	−102	35	33	34	47
	−159		−158	−159	−158	−151
	−81		−82	−81	−82	−89
D-Trp^{8}	6.2 Hz	6.1 Hz	6.5 Hz	4.4 Hz	6.4 Hz	5.8 Hz
	−32	−31	−35	−18	−34	−29
	−88	−89	−85	−102	−86	−91
	80	79	82	69	81	77
	160	161[a]	158	171[a]	159	163
Lys^{9}	8.5 Hz	8.46 Hz	7.8 Hz	8.62 Hz	6.2 Hz	8.4 Hz
	−144	−144	69	−143	88	−145
	−96	−96	51	−97	32	−95
			−149		−160	
			−91		−80	
Thr^{10}	9.2 Hz	6.11 Hz	9.9 Hz	9.2 Hz	8.2 Hz	8.8 Hz
	−137	89	−127	−138	−146	−142
	−102	31	−112	−102	−94	−98
		−161				
		−79				

[a] Values were calculated using $J_{\text{NH-C}\alpha\text{H}} = A\cos^2|\phi \pm 60°| - B\cos|\phi \pm 60°| + C$, where (+) is for a D-configuration, (−) is for a L-configuration and the values are those proposed by Bystrov *et al.* for a chiral residue [29].

spanning the D-Trp^{8} and Lys^{9} residues. No other NH-NH NOEs have been observed, suggesting the presence of type II′ β-turns with D-Trp^{8} in the $i+1$ position which is also supported by the low temperature coefficients of the Thr^{10}NH in the **Nphe^{6}-Nal^{7}** analog **1** and the **Nnal^{6}** compound **3**, strong sequential NOEs between D-Trp^{10}H$^{\alpha}$ and Lys^{9}NH and medium NOEs between Lys^{9}NH and Lys^{9}H$^{\alpha}$. The relatively high temperature coefficient of the Thr^{10}HN in the **Nal^{11}-Nphe^{6}** analog **2** suggests that the type II′ β-turn in the *trans* isomer of this compound is not as stable as in the other two analogs. However, the similarity in all other NMR data still suggests that the backbone conformation is not considerable different from the **Nphe^{6}-Nal^{7}** analog **1** and the **Nnal^{6}** compound **3**.

The low temperature coefficients of the NH protons in position 7 suggest that these protons are involved in the second turn of the cyclic hexapeptides, which can be a β-turn with Xaa^{11} in the $i+1$ position or γ-turn about the peptoid residue. Based upon the NMR data, the nature of the second turn cannot be determined unambiguously due to the N-substituted structure of the peptoid residues.

As seen for the *cis* isomer, the bulky Nal group in position 7 causes a close spatial proximity between the D-Trp and Lys side chain for the **Nphe^{6}-Nal^{7}** analog **1**. Again, several NOEs can be observed which prove the short distance between these two side chains, such as a weak NOE between the D-Trp aromatic NH proton and the Lys ε-proton.

Table 3 Temperature Coefficients of *c*-[Phe[11]-Nphe[6]-Nal[7]-D-Trp[8]-Lys[9]-Thr[10]] (**1**), *c*-[Nal[11]-Nphe[6]-Phe[7]-D-Trp[8]-Lys[9]-Thr[10]] (**2**), *c*-[Phel[11]-Nnal[6]-Phe[7]-D-Trp[8]-Lys[9]-Thr[10]] (**3**) in ppb/K

Xaa^6-Xbb^7	Phe^{11}-$Nphe^6$-Nal^7		Nal^{11}-$Nphe^6$-Phe^7		Phe^{11}-$Nnal^6$-Phe^7	
	cis	*trans*	*cis*	*trans*	*cis*	*trans*
Xaa^{11}	4.6	2.1	4.1	0.7	4.5	2.4
Xbb^7	4.2	0.7	2.3	0.8	3.6	1.3
D-Trp^8	6.8	7.3	4.8	5.6	4.3	5.3
Lys^9	4.3	4.4	4.9	4.0	4.8	3.5
Thr^{10}	−0.7	1.3	0.5	2.6	0.9	1.7

Molecular Modeling

The conformational search using distance geometry, 1000 K molecular dynamics simulations and cluster analysis of the *cis* isomers of compounds **1**–**3** resulted in two highly populated conformational families for each compound. For the **Nphe⁶-Nal⁷** analog **1** and the **Nnal⁶** analog **3** a family of 'folded' conformations (**cisa**) as the lowest energy cluster and 'flat' conformations (**cisb**), slightly higher in energy, were obtained. For the **Nphe⁶-Nal⁷** analog **1**, the 'folded' conformation was higher populated and lower in energy than the 'flat' conformation. The opposite result was obtained for the **Nnal⁶** compound **3**. The structures obtained for this compound also showed larger γ-turn distortions of the β-turn than the other two compounds. Finally, no 'flat' conformation was obtained for the **Nal¹¹-Nphe⁶** analog **2**. The structures **cisa** and **cisb** obtained for this analog are both 'folded': the higher populated conformation **cisa** is 'folded' with a γ-turn conformation about Thr^{10} and Phe^7; the less populated conformation **cisb** is only 'folded' about Thr^{10}, but not about Phe^7.

The torsional angles of the lowest energy conformations of each cluster of the three analogs are given in Table 5. All these structures exhibit very similar backbone conformations containing a well defined type II′ β-turn with D-Trp in the $i+1$ position and a type VI*a* β-turn spanning Phe^{11} and the peptoid residue. The main differences in the torsional angles between the two structures obtained for each compound are the ϕ and ψ angles of residues Xaa^7 and Thr^{10}. The 'folded' conformations are characterized by γ-turn conformations about these two residues which lead to torsional angles of approximately −85° (ϕ) and 80° (ψ). These values correspond to γ-turns about residues 7 and 10. In the 'flat' conformations of the **Nphe⁶-Nal⁷** analog **1** and the **Nnal⁶** compound **3**, these values are considerably different and the residues 7 and 10 have ϕ angles of approximately −155° and ψ-angles around −125°. The 'folded' conformations **cisa** are in good agreement with all experimental data, whereas the 'flat' conformations **cisb** for the **Nphe⁶-Nal⁷** analog **1** and the **Nnal⁶** compound **3** violate the D-Trp^8NH-Nal^7NH and Phe^{11}NH-Thr^{10}NH NOEs (see Figure 1). The NOE between D-Trp^8HN and Thr^{10}HN observable for the **Nnal⁶** compound **3** is severely violated in both structures and suggests the presence of a second conformation which lacks the type II′ β-turn with D-Trp in the $i+1$ position. Both conformational families found for the **Nal¹¹-Nphe⁶** analog **2**, **cisa** and **cisb**, satisfy all experimental data. In general, the observation of the D-Trp^8NH-Nal^7NH and Phe^{11}NH-Thr^{10}NH NOEs points towards the 'folded' conformation. This is illustrated in Figure 1: in the 'folded' structure (**a**) these distances are 3.8 and 3.6, while they are 4.3 and 4.2 in the 'flat' conformation (**b**). Figure 1**c** demonstrates that the NOE between Xaa^7HN and D-TrpHN is also satisfied by a conformation in which the type II′ γ-turn is lost and the peptide bond between Xaa^7 and D-Trp^8 are turned outside the ring thus allowing close spatial proximity between the Xaa^7HN and D-Trp^8HN. This arrangement, however, leads also to a close spatial proximity between the D-Trp^8HN and the Thr^{10}HN as illustrated in Figure 1**c**. No such NOE was observed for the **Nphe⁶-Nal⁷** analog **1** and the **Nal¹¹-Nphe⁶** analog **2** but was observable for the **Nnal⁶** compound **3**.

The 'folded' conformation **cisa** of each of the analogs was subjected to distance restrained and free molecular dynamics simulations at 300 K. The average torsional angles and RMSD values during the molecular dynamics simulations are given in Table 6. Distance restrained molecular dynamics of

Table 4 $J_{(CH^{\alpha}\text{-}CH^{\beta})}$ Coupling Constants (in Hz) and Calculated Side Chain Populations of *c*-[Phe[11]-Nphe[6]-Nal[7]-D-Trp[8]-Lys[9]-Thr[10]] (**1**), *c*-[Nal[11]-Nphe[6]-Phe[7]-D-Trp[8]-Lys[9]-Thr[10]] (**2**), *c*-[Phe[11]-Nnal[6]-Phe[7]-D-Trp[8]-Lys[9]-Thr[10]] (**3**)[a]

Xaa[6]-Xbb[7]	Phe[11]-Nphe[6]-Nal[7]		Nal[11]-Nphe[6]-Phe[7]		Phe[11]-Nnal-Phe[7]	
	cis	*trans*	*cis*	*trans*	*cis*	*trans*
Xaa[11]	β^{l}: 6.0	β: 6.8	β^{l}: 5.4	–[c]	β^{l}: 6.7	–[c]
	β^{h}: 6.3	β: 6.8	β^{h}: 10.3	–	β^{h}: 6.7	–
	$f(g^-)0.27$	$f(g^-)=0.32$	$f(g^-)=0.18$	–	$f(g^-)=0.30$	–
	$f(t)=0.24$	$f(t)=0.32$	$f(t)=0.65$	–	$f(t)=0.30$	–
	$f(g^+)=0.49$	$f(g^+)=0.36$	$f(g^+)=0.17$	–	$f(g^+)=0.40$	–
Xaa[7]	β^{l}: 3.8	β^{l}: 3.9	β^{l}: 6.7	β^{l}: 6.9	β^{l}: 5.8	β^{l}: 5.4
	β^{h}: 6.8	β^{h}: 9.3	β^{h}: 6.9	β^{h}: 8.3	β^{h}: 6.7	β^{h}: 6.2
	$f(g^-)=0.26, 0.02$	$f(g^-)=0.56$	$f(g^-)=0.31$	$f(g^-)=0.33$	$f(g^-)=0.31$	$f(g^-)=026, 0.18$
	$f(t)=0.26, 0.02$	$f(t)=0.03$	$f(t)=0.32$	$f(t)=0.46$	$f(t)=0.22$	$f(t)=0.18, 0.26$
	$f(g^+)=0.72$	$f(g^+)=0.41$	$f(g^+)=0.37$	$f(g^+)=0.21$	$f(g^+)=0.47$	$f(g^+)=0.56$
D-Trp[8]	β^{l}: 9.2	β^{l}: 9.5	β^{l}: 8.5	β^{l}: 8.5	β^{l}: 7.1	β^{l}: 6.9
	β^{h}: 6.1	β^{h}: 6.0	β^{h}: 7.1	β^{h}: 7.2	β^{h}: 7.1	β^{h}: 7.1
	$f(g^-)=0.20$	$f(g^-)=0.17$	$f(g^-)=0.34$	$f(g^-)=0.35$	$f(g^-)=0.34$	$f(g^-)=0.34$
	$f(t)=0.55$	$f(t)=0.58$	$f(t)=0.48$	$f(t)=0.48$	$f(t)=0.34$	$f(t)=0.33$
	$f(g^+)=0.25$	$f(g^+)=0.20$	$f(g^+)=0.18$	$f(g^+)=0.17$	$f(g^+)=0.32$	$f(g^+)=0.33$
Lys[9]	β^{l}: 3.5[b]	β^{l}: 4.5	β^{l}: 3.3	β^{l}: 3.2	β^{l}: 3.2	β^{l}: 4.7
	β^{h}: 11.8	β^{h}: 11.3	β^{h}: 11.4	β^{h}: 11.1	β^{h}: 11.2	β^{h}: 10.8
	$f(g^-)=0.84$	$f(g^-)=0.80$	$f(g^-)=0.80$	$f(g^-)=0.78$	$f(g^-)=0.78$	$f(g^-)=0.75$
	$f(t)=0.08$	$f(t)=0.15$	$f(t)=0.06$	$f(t)=0.06$	$f(t)=0.05$	$f(t)=0.19$
	$f(g^+)=0.08$	$f(g^+)=0.05$	$f(g^+)=0.14$	$f(g^+)=0.16$	$f(g^+)=0.17$	$f(g^+)=0.06$
Thr[10]	β: 4.1	β: 4.7	β: 4.5	β: 4.3	β: 4.4	β: 4.7
	$f(g^+, t)=0.86$	$f(g^+, t)=0.81$	$f(g^+, t)=0.83$	$f(g^+, t)=0.84$	$f(g^+, t)=0.84$	$f(g^+, t)=0.81$
	$f(g^-, t)=0.14$	$f(g^-, t)=0.19$	$f(g^-, t)=0.17$	$f(g^-, t)=0.16$	$f(g^-, t)=0.16$	$f(g^-, t)=0.19$

[a] Values were calculated using $J_T = 13.56$ and $J_G = 2.60$ Hz for non-aromatic side chains, $J_T = 13.85$ and $J_G = 2.55$ Hz for aromatic side chains [31,32].
[b] From DQF-COSY.
[c] J is not measurable.

the **Nphe[6]-Nal[7]** analog **1** and the **Nal[11]-Nphe[6]** analog **2** resulted in two highly populated conformations for each compound. The lowest energy conformations are structures with a well defined type II′ β-turn about D-Trp[8] and Lys[9], a type VI*a* β-turn in the bridging region and γ-turn conformations about residues 10 and 7. These structures were in excellent agreement with the experimental data. The second conformational family with high population are ‘flat’ structures with respect to the conformations about residues 10 and 7 and these structures show considerable distortions in the type II′ β-turn. These conformations violate the ϕ angle of D-Trp[8] as determined from the $J_{NH\text{-}C^{\alpha}H}$ and they do not account for the low temperature coefficient of Thr[10]HN because the peptide bond between Xaa[7] and D-Trp[8] is turned outside the ring and the hydrogen bond between the ThrHN and Xaa[7]O is broken. The ϕ angle of D-Trp[8] is considerably different from that observed in a type II′ β-turn (130°). During restrained molecular dynamics simulations, the ‘flat’ conformation with the distorted type II′ β-turn had insignificant populations for the **Nphe[6]-Nal[7]** analog **1** and the **Nal[11]-Nphe[6]** analog **2** but was the predominant conformation for the **Nnal[6]** compound **3**. In the absence of distance constraints, the ‘folded’ conformations of the **Nphe[6]-Nal[7]** analog **1** and the **Nal[11]-Nphe[6]** analog **2** are very stable and no ‘flat’ structures were observed. The type II′ β-turn is very well defined and the structures are in agreement with all experimental data. Contrary to that, the distorted ‘flat’ conformation was predominant for

Table 5 Backbone Torsion Angles for *cis* and *trans* Isomers of *c*-[Phe[11]-Nphe[6]-Nal[7]-D-Trp[8]-Lys[9]-Thr[10]] (**1**), *c*-[Nal[11]-Nphe[6]-Phe[7]-D-Trp[8]-Lys[9]-Thr[10]] (**2**) and *c*-[Phe[11]-Nnal[6]-Phe[7]-D-Trp[8]-Lys[9]-Thr[10]] (**3**)

Structure		Xaa[11]	Nxbb[6]	Xcc[7]	D-Trp[8]	Lys[9]	Thr[10]
c-[Phe[11]-Nphe[6]-Nal[7]-D-Trp[8]-Lys[9]-Thr[10]] (**1**)							
cisa	ϕ	−58	−84	−85	62	−72	−83
	ψ	140	4	84	−134	−22	73
	ω	3	−178	−175	179	179	−161
	χ_1	−78	96	−172	177	−64	−58
cisb	ϕ	−58	−109	−158	73	−88	−156
	ψ	131	38	125	−126	15	128
	ω	13	177	170	−176	176	−176
	χ_1	−177	97	179	170	−54	−70
transa	ϕ	−57	97	−161	78	−81	−135
	ψ	143	−53	134	−132	12	165
	ω	−178	170	164	−180	167	−171
	χ_1	54	−101	180	172	64	−171
transb	ϕ	50	88	−80	59	−78	−89
	ψ	75	−46	83	−127	−11	74
	ω	−178	−178	−165	175	−175	178
	χ_1	−168	68	−173	177	−63	−58
c-[Nal[11]-Nphe[6]-Phe[7]-D-Trp[8]-Lys[9]-Thr[10]] (**2**)							
cisa	ϕ	−35	−79	−86	62	−60	−90
	ψ	131	−1	79	−126	−37	65
	ω	3	−178	−175	179	179	−172
	χ_1	−179	−119	−173	172	−75	58
cisb	ϕ	87	128	−158	82	−78	−87
	ψ	−92	−69	89	−133	−20	70
	ω	1	177	179	180	176	−176
	χ_1	−166	−94	51	−176	−172	54
trans	ϕ	−54	99	−163	78	−83	−152
	ψ	139	−65	148	119	2	178
	ω	−176	175	162	−178	177	−179
	χ_1	−54	141	172	174	−59	164
c-[Phe[11]-Nnal[6]-Phe[7]-D-Trp[8]-Lys[9]-Thr[10]] (**3**)							
cisa	ϕ	−59	−105	−158	78	−84	−159
	ψ	127	19	136	−137	20	126
	ω	18	−179	177	179	178	−178
	χ_1	−177	132	−176	174	−520	−70
cisb	ϕ	−68	−86	−84	65	−70	−82
	ψ	140	4	78	−129	−31	75
	ω	11	179	−177	173	171	−162
	χ_1	50	125	−171	170	−64	−58
transa	ϕ	−62	102	−134	79	−72	−86
	ψ	126	−39	69	−96	−41	152
	ω	−174	177	158	177	165	−175
	χ_1	−55	69	63	173	−168	−66
transb	ϕ	51	71	−87	78	−104	−159
	ψ	60	−24	66	−86	1	125
	ω	−178	−171	179	−173	−178	−177
	χ_1	−66	−91	−63	171	−66	−72

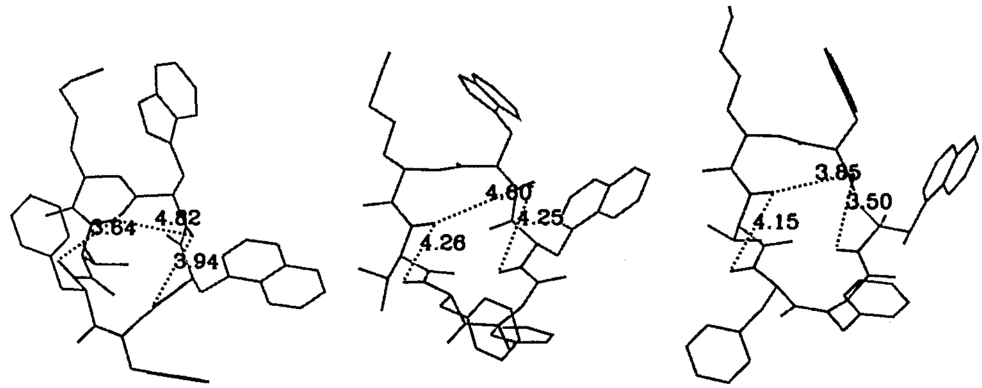

Figure 1 Distances between D-Trp^{8}HN-Xaa^{7}HN-Thr^{10}HN-Xaa^{11}HN and D-Trp^{8}HN-Thr^{10}HN in the 'folded' conformation (**a**), a 'flat' conformation containing a type II′ β-turn (**b**) and a 'flat' conformation with a distorted type II′ β-turn (**c**).

the **Nnal^{6}** compound **3** even in the absence of distance constraints.

Figure 2 gives the distances ThrHN-Phe^{7}O, and Nal^{11}-LysO during 300 K free molecular dynamics simulations of the **Nal^{11}-Nphe^{6}** analog **2**. A correlation between the 'folding' of the structure and the hydrogen bond within the type II′ β-turn is obvious.

In general, the molecular dynamics simulations suggested that the overall backbone structure of the **Nphe^{6}-Nal^{7}** analog **1** and the **Nal^{11}-Nphe^{6}** analog **2** is very rigid. The average torsional angles and RMSD values for distance restrained and free molecular dynamics simulations of the *cis* isomers are given in Table 6. The RMSD values of the backbone torsion angles are very small indicating that the flexibility of the molecule is very low.

The molecular dynamics simulations of the **Nnal^{6}** compound **3** indicated that this molecule is by far more flexible than the **Nphe^{6}-Nal^{7}** analog **1** and the **Nal^{11}-Nphe^{6}** analog **2**. Furthermore, γ-turn-like distortions of the β-turn occur more easily than in the **Nphe^{6}-Nal^{7}** analog **1** and the **Nal^{11}-Nphe^{6}** analog **2**. The regions with the greatest flexibility in the restrained MD at 300 K are ϕ(Phe^{11}), ψ(Nnal^{6}), ϕ(D-Trp^{8}), ψ(Lys^{9}) and ψ(Thr^{10}). The Nnal^{6} residue is not as rigid as was expected and adopts χ^{1}values of 115° to 125°, $-96°$ to $-71°$ and 60° to 80°.

Figure 3 shows the distances of Thr^{10}HN-Phe^{7}O and Phe^{11}HN-Lys^{9}O during free and restrained molecular dynamics simulations of the **Nnal^{6}** compound **3** at 300 K.

For the *trans* isomers of the **Nphe^{6}-Nal^{7}** analog **1** and the **Nnal^{6}** compound **3**, two major conformational families were obtained from distance geometry, 1000 K molecular dynamics simulations and cluster analysis. Both conformations contain a type II′ β-turn with D-Trp^{8} in the $i+1$ position. The 'flat' conformations (**transa**) adopt a type II′ β-turn with Phe^{11} in the $i+1$ position and the 'folded' conformations (**transb**) contain a second β-turn around Phe^{11} and Nxaa^{6}. Superimposition of ideal type I, type II and type III β-turns with this part of the molecule resulted in RMSD values of 0.76, 0.96 and 0.80 for the **Nphe^{6}-Nal^{7}** analog **1** and 1.57, 1.05 and 1.56 for the **Nnal^{6}** compound **3**. For the **Nal^{11}-Nphe^{6}** analog **2** only one major conformational family was obtained. This conformational family contains a type II′ β-turn with D-Trp^{8} in the $i+1$ position and a highly distorted type II′ β-turn in the bridging region. This structure is 'flat' and very similar to structures **transa** found for the **Nphe^{6}-Nal^{7}** analog **1** and the **Nnal^{6}** compound **3**. The torsional angles of the *trans* isomers found for our compounds are given in Table 5.

The distance restrained molecular dynamics simulations of the *trans* isomers showed that these isomers are considerably more flexible than the *cis* isomers (Table 7). In general, the regions of highest backbone flexibility are the torsion angles ϕ^{11}, ψ^{11}, ϕ^{7} ψ^{9} and ϕ^{10}. As indicated by the high flexibility in the torsional angle ψ^{9}, γ-turn-like distortions of the type II′ β-turn with D-Trp^{8} in the $i+1$ occur easily. This is experimentally supported by the high temperature coefficients of the Thr^{10}HN protons. As far as the second turn is concerned, the majority of structures showed a slightly distorted type II β-turn with Phe^{11} in the $i+1$ position. For the **Nphe^{6}-Nal^{7}** analog **1**, 'folded' structures with a γ-turn conformation about residues 10 and 7 are predominant, while mainly 'flat' conformations were obtained for

Table 6 Torsion Angles and RMSD Values for *cis* Isomers of *c*-[Phe[11]-Nphe[6]-Nal[7]-D-Trp[8]-Lys[9]-Thr[10]] (**1**), *c*-[Nal[11]-Nphe[6]-Phe[7]-D-Trp[8]-Lys[9]-Thr[10]] (**2**) and *c*-[Phe[11]-Nnal[6]-Phe[7]-D-Trp[8]-Lys[9]-Thr[10]] (**3**) during Restrained (RMD) and Free (FMD) Molecular Dynamics Simulations Over a Period of 300 ps

MD		Xaa[11]	Nxbb[6]	Xcc[7]	D-Trp[8]	Lys[9]	Thr[10]
c-[Phe[11]-Nphe[6]-Nal[7]-D-Trp[8]-Lys[9]-Thr[10]] (**1**)							
300 K RMD	ϕ	−69 (8)	−113 (4)	−174 (5)	117 (7)	−90 (2)	−153 (5)
	ψ	138 (6)	50 (5)	105 (3)	−134 (4)	26 (3)	138 (14)
	ω	4 (3)	175 (1)	164 (2)	169 (2)	178 (1)	179 (6)
	χ_1	−13 (68)	98 (79)	175 (1)	169 (1)	−60 (3)	58 (3)
300 K FMD	ϕ	−65 (12)	−94 (13)	−139 (30)	87 (33)	−72 (10)	−88 (17)
	ψ	141 (2)	22 (55)	100 (19)	−134 (10)	−40 (12)	110 (44)
	ω	9 (3)	179 (5)	−179 (4)	−177 (6)	173 (2)	−176 (9)
	χ_1	−64 (1)	95 (8)	−179 (2)	−177 (3)	−1 (109)	58 (4)
c-[Nal[11]-Nphe[6]-Phe[7]-D-Trp[8]-Lys[9]-Thr[10]] (**2**)							
300 K RMD	ϕ	−67 (2)	−101 (2)	−105 (12)	85 (14)	−69 (1)	−79 (5)
	ψ	143 (1)	18 (6)	74 (4)	−128 (2)	−47 (1)	104 (11)
	ω	7 (2)	178 (1)	172 (1)	−173 (3)	171 (1)	−169 (4)
	χ_1	−55 (0)	−86 (21)	−176 (0)	176 (0)	−65 (0)	56 (1)
300 K FMD	ϕ	−60 (5)	−93 (13)	−133 (32)	78 (21)	−67 (1)	−86 (7)
	ψ	139 (1)	25 (46)	90 (12)	−133 (2)	−43 (3)	92 (25)
	ω	12 (1)	−178 (5)	175 (5)	−174 (4)	175 (1)	−175 (5)
	χ_1	−57 (1)	95 (4)	−179 (0)	177 (0)	−106 (55)	56 (2)
c-[Phe[11]-Nnal[6]-Phe[7]-D-Trp[8]-Lys[9]-Thr[10]] (**3**)							
300 K RMD	ϕ	−75 (29)	−93 (10)	−149 (28)	133 (37)	−71 (7)	−125 (17)
	ψ	136 (5)	8 (36)	79 (31)	−125 (16)	−20 (25)	83 (94)
	ω	15 (10)	179 (5)	174 (6)	176 (6)	172 (3)	−174 (10)
	χ_1	−64 (1)	119 (67)	139 (63)	178 (3)	−30 (70)	55 (2)
300 K FMD	ϕ	−82 (40)	−81 (9)	−128 (33)	130 (35)	−73 (15)	−105 (27)
	ψ	139 (6)	−52 (55)	114 (29)	−126 (14)	−51 (27)	179 (74)
	ω	9 (10)	−173 (6)	−178 (6)	−178 (2)	175 (5)	172 (7)
	χ_1	52 (41)	115 (19)	−72 (44)	176 (2)	−8 (61)	60 (4)

the **Nal[11]-Nphe[6]** analog **2**. As seen for the *cis* isomer, the **Nnal[6]** compound **3** exhibits more flexibility in the type II′ β-turn region compared with the other analogs.

DISCUSSION

The results of the conformational analysis of the *cis* isomers of our compounds demonstrate that the **Nphe[6]-Nal[7]** analog **1** and the **Nnal[6]** compound **3** can adopt 'folded' and 'flat' backbone conformations. Only 'folded' conformations are accessible for the **Nal[11]-Nphe[6]** analog **2**. Both structures contain a type II′ β-turn with D-Trp[8] in the $i+1$ position and a type VI*a* β-turn in the bridging region. The 'folded' conformations are in good agreement with the experimental data, whereas the 'flat' conformations violate the HN[7]-HN[8] and HN[10]-HN[11] NOEs. Computer simulations of the *cis* isomers of the **Nphe[6]-Nal[7]** analog **1** and the **Nal[11]-Nphe[6]** analog **2** have shown that these NOEs clearly favor the 'folded' conformation over the 'flat' conformation since they can only be satisfied by a 'folded' type II′ β-turn conformation or by a 'flat' conformation in which the type II′ β-turn with D-Trp[8] in the $i+1$ position is severely distorted. The distorted structures, however, violate other experimental data such as the ϕ angle of D-Trp[8] and the low temperature coefficient of Thr[10]HN. The superimposed structures of the 'folded' conformations which are believed to be the bioactive conformations are shown in Figure 4. This demonstrates that the overall backbone conformations of these three structures are identical and that the main differences between these conformations is the orientation of the Nnal residue in the **Nnal[6]** compound **3** compared with the Nphe residue in the **Nphe[6]-Nal[7]** analog **1** and the **Nal[11]-Nphe[6]** analog **2**.

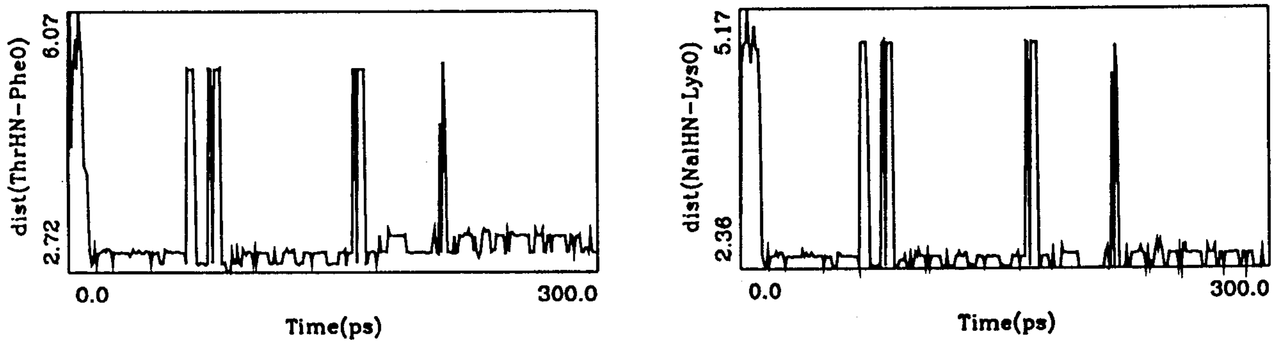

Figure 2 Free molecular dynamics simulations of the *cis* isomer of *c*-[Na^{11}-Nphe^{6}-Phe^{7}-D-Trp^{8}-Lys^{9}-Thr^{10}] (analog **2**) showing the distances between Thr^{10}HN-Phe^{7}O and Na^{11}HN-Lys^{9}O. The distance Thr^{10}HN-Phe^{7}O represents the hydrogen bond within the type II′ β-turn with D-Trp in the $i+1$ position. The distance Na^{11}HN-Lys^{9}O represents the hydrogen bond within one of two γ-turns which are present in the 'folded' conformation but not in the 'flat' conformation (the other hydrogen bond of the 'folded' conformation is between D-Trp^{8}HN and Nphe^{6}O).

The peptoid residue in the **Nnal^{6}** analog **3** is oriented towards the Phe^{7} residue, while in the **Nphe^{6}-Nal^{7}** analog **1** and the **Nal^{11}-Nphe^{6}** analog **2** the peptoid residue is oriented towards residue 11. Our studies have also shown that the backbone structure of all three molecules is considerably more rigid than that of the **Nphe^{6}** analog of L-363,301. This is especially true for the two analogs containing Nal in either positions 7 or 11.

The other main difference in the *cis* isomers of the three analogs is the behavior during restrained and free molecular dynamics at 300 K. Figure 5 presents the ϕ plots for the residues D-Trp^{8} and Lys^{9} of the **Nphe^{6}-Nal^{7}** (a) and the **Nnal^{6}** (b) analogs during free molecular dynamics simulation at 300 K. These results clearly demonstrate that this region in the **Nnal^{6}** analog is more flexible and that the type II′ β-turn is less stable compared with the **Nphe^{6}-Nal^{7}** analog (similar results as for the **Nphe^{6}-Nal^{7}** analog were obtained for the **Nal^{11}-Nphe^{6}** analog). This result is also supported by a medium NOE between Thr^{10}HN and D-Trp^{8}HN which is not consistent with a type II′ β-turn. Other experimental data such as the temperature coefficient of Thr^{10}HN, however, indicate that the type II′ β-turn structure is highly populated in the **Nnal^{6}** analog. Although the NMR data of all three compounds are very similar, the NOE between Thr^{10}HN and Trp^{8}HN observed for the **Nnal^{6}** compound **3** and the behavior of this analog during molecular dynamics simulations compared with the **Nphe^{6}-Nal^{7}** analog **1** and the **Nal^{11}-Nphe^{6}** analog **2** implies the existence of a second conformation for this analog in which the type II′ β-turn is lost. Figure 6 shows the major conformational clusters which were obtained as result of free molecular dynamics. The free molecular dynamic simulation of the **Nphe^{6}-Nal^{7}** analog **1** and the **Nal^{11}-Nphe^{6}** analog **2** resulted in 240 or 270 'folded' structures (out of 300 structures obtained during the 300 ps) with very similar backbone conformations and side chain orientations. The same simulation for the **Nnal^{6}** analog resulted in 74 'folded' structures and 130 'flat' structures (out of 300). In the 'flat' structures the Nnal^{6} residue adopts a side chain orientation which leads to a close spatial proximity of the Nnal^{6} residue and the Phe^{7}, Thr^{10} and even the D-Trp^{8} side chain. This proximity and the resulting steric interaction give a possible explanation for the enhanced flexibility of the type II′ β-turn in the Nnal analog and the distortions observed in this region of the molecule. Since this turn is crucial for the bioactivity, the reduced binding activity of the Nnal analog can be connected with the flexibility of the molecule in the β-turn region. In this series of compounds, the bulky Nal group in positions 7 or 11 or the Nnal group in position 6 seems to prevent the formation of a 'flat' conformation with a well defined type II′ β-turn. Whenever a 'flat' conformation was observed, there was a distortion of the type II′ β-turn. The Xaa^{7}C=O was turned outside the ring and the hydrogen bond between the Thr^{10}HN and Xaa^{7}O was broken.

Our results show that the introduction of the Nal residue in position 11 or 7 leads to compounds with very rigid backbone and side chain conformations containing a type II′ β-turn with D-Trp^{8} in the $i+1$ position and a type VI β-turn spanning residues 11 and 6. The compounds bind effectively to the hsst2, hsst3 and hsst5 receptors. Contrary to that, the introduction of the Nnal residue in position 6 leads

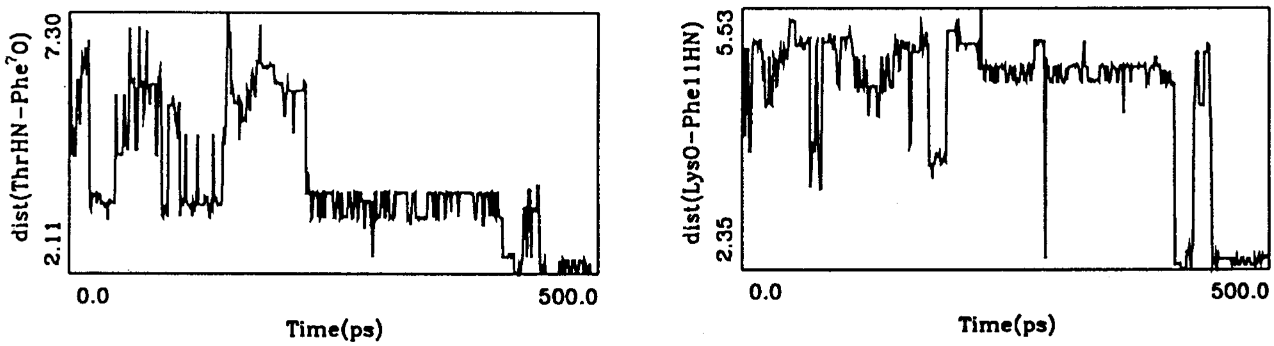

Figure 3 Free molecular dynamics simulations of the *cis* isomer of *c*-[Phe^{11}-Nnal^{6}-Phe^{7}-D-Trp^{8}-Lys^{9}-Thr^{10}] (analog **3**) showing the distances between Thr^{10}HN-Phe^{7}O and Phe^{11}HN-Lys^{9}O. The distance Thr^{10}HN-Phe^{7}O represents the hydrogen bond within the type II′ β-turn with D-Trp in the $i+1$ position while the distance Phe^{11}HN-Lys^{9}O represents the hydrogen bond within one of two γ-turns which are present in the 'folded' conformation but not in the 'flat' conformation.

Table 7 Torsion Angles and RMSD Values for *trans* Isomer of *c*-[Phe^{11}-Nphe^{6}-Nal^{7}-D-Trp^{8}-Lys^{9}-Thr^{10}] (**1**), *c*-[Na^{11}-Nphe^{6}-Phe^{7}-D-Trp^{8}-Lys^{9}-Thr^{10}] (**2**) and *c*-[Phe^{11}-Nnal^{6}-Phe^{7}-D-Trp^{8}-Lys^{9}-Thr^{10}] (**3**) during Restrained (RMD) and Free (FMD) Molecular Dynamics Simulations Over a Period of 300 ps

MD		Xaa^{11}	Nxbb^{6}	Xcc^{7}	Trp	Lys	Thr
c-[Phe^{11}-Nphe^{6}-Nal^{7}-D-Trp^{8}-Lys^{9}-Thr^{10}] (**1**)							
300 K RMD	ϕ	−32 (59)	102 (9)	−144 (37)	86 (16)	−77 (20)	−95 (38)
	ψ	125 (31)	−64 (15)	127 (8)	−146 (7)	−22 (39)	134 (30)
	ω	176 (6)	175 (6)	177 (3)	177 (3)	174 (5)	177 (3)
	χ_1	−112 (56)	−111 (62)	179 (1)	−50 (51)	−63 (2)	−151 (48)
300 K FMD	ϕ	68 (36)	93 (9)	−97 (33)	82 (36)	−89 (18)	−141 (21)
	ψ	88 (13)	−81 (15)	118 (15)	−148 (10)	17 (46)	91 (48)
	ω	168 (7)	−176 (2)	−177 (5)	174 (6)	−178 (5)	173 (5)
	χ_1	−173 (2)	−65 (91)	179 (2)	−59 (21)	−61 (2)	−59 (3)
c-[Nal^{11}-Nphe^{6}-Phe^{7}-D-Trp^{8}-Lys^{9}-Thr^{10}] (**2**)							
300 K RMD	ϕ	18 (70)	88 (15)	−89 (42)	121 (31)	−107 (35)	−126 (29)
	ψ	100 (26)	−138 (53)	130 (7)	−119 (21)	−38 (27)	166 (39)
	ω	178 (5)	−177 (3)	178 (9)	−179 (4)	173 (5)	−176 (4)
	χ_1	−58 (2)	−136 (48)	−179 (2)	164 (39)	45 (50)	−172 (4)
300 K FMD	ϕ	−66 (5)	108 (8)	−142 (18)	84 (9)	−71 (1)	−64 (3)
	ψ	137 (5)	−53 (6)	93 (26)	−128 (4)	−49 (1)	141 (13)
	ω	−174 (5)	−179 (6)	169 (3)	−173 (2)	168 (5)	−173 (10)
	χ_1	−54 (18)	−142 (77)	−99 (58)	177 (1)	−65 (11)	−172 (3)
c-[Phe^{11}-Nnal^{6}-Phe^{7}-D-Trp^{8}-Lys^{9}-Thr^{10}] (**3**)							
300 K RMD	ϕ	75 (4)	86 (15)	−114 (52)	155 (11)	−109 (44)	−129 (23)
	ψ	80 (5)	−114 (47)	−114 (10)	−118 (14)	−61 (5)	153 (9)
	ω	165 (8)	179 (2)	−177 (1)	176 (6)	169 (8)	178 (4)
	χ_1	−56 (1)	−122 (25)	179 (0)	−177 (2)	−169 (47)	−5 (53)
300 K FMD	ϕ	88 (41)	43 (69)	−76 (22)	142 (18)	−137 (33)	−101 (39)
	ψ	111 (26)	−130 (68)	113 (17)	−11 (21)	−70 (45)	115 (21)
	ω	178 (5)	178 (6)	−170 (7)	179 (5)	168 (15)	−174 (3)
	χ_1	−78 (55)	−100 (43)	−78 (48)	179 (3)	102 (65)	−61 (2)

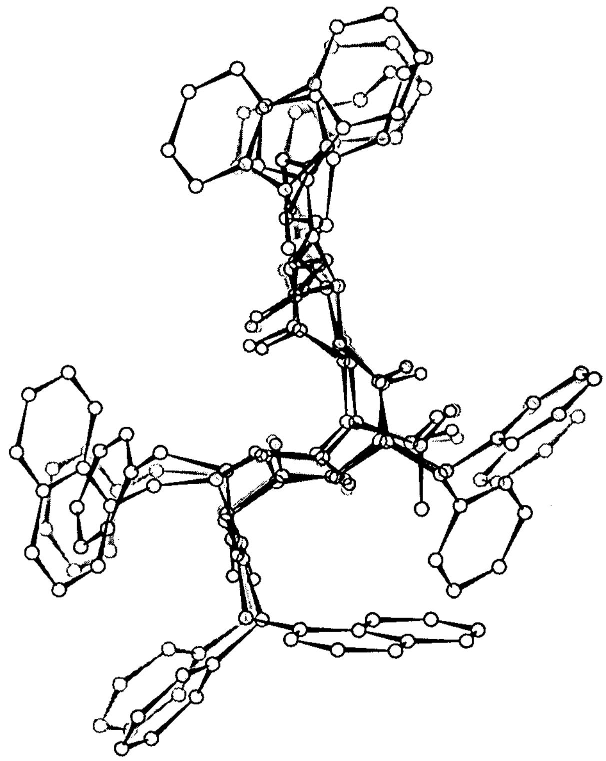

Figure 4 Superimposed structures of the 'folded' conformations of the *cis* isomers of *c*-[Phe^{11}-Nphe^{6}-Nal^{7}-D-Trp^{8}-Lys^{9}-Thr^{10}] **1** (light), *c*-[Nal^{11}-Nphe^{6}-Phe^{7}-D-Trp^{8}-Lys^{9}-Thr^{10}] **2** (gray) and *c*-[Phe^{11}-Nnal^{6}-Phe^{7}-D-Trp^{8}-Lys^{9}-Thr^{10}] **3** (black).

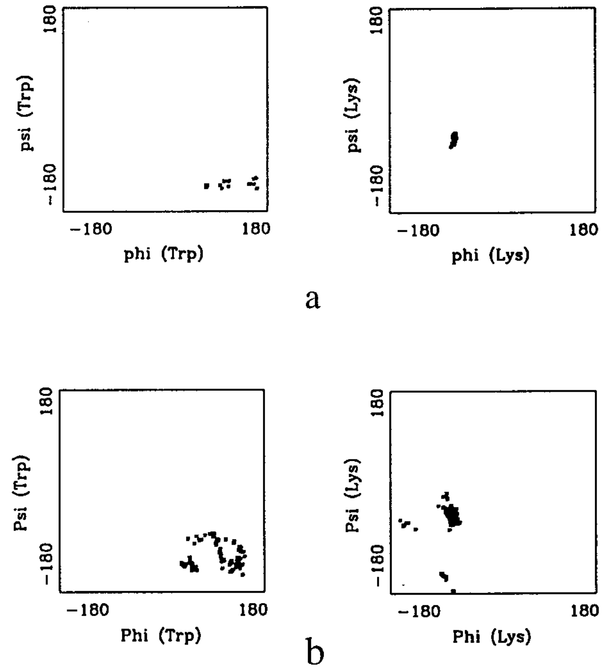

Figure 5 Plots of the ϕ and ψ torsional angles of D-Trp^{8} and Lys^{9} during free molecular dynamics simulations at 300 K of compounds *c*-[Phe^{11}-Nphe^{6}-Nal^{7}-D-Trp^{8}-Lys^{9}-Thr^{10}] (**Nphe^{6}-Nal^{7}** analog, **1**) (a) and *c*-[Phe^{11}-Nal^{6}-Phe^{7}-D-Trp^{8}-Lys^{9}-Thr^{10}] (**Nnal^{6}** analog, **3**) (b).

to conformations in which the peptoid side chain can interfere with the residues within the type II′ β-turn. This leads to a distortion of the β-turn structure and subsequently to a decrease in activity. This analog shows 6-fold reduced binding activity to the hsst2 receptor and 40 times weaker binding to the hsst5 compared with L-363,301 and has no detectable binding affinity to the other receptors. However, despite its low binding affinity to

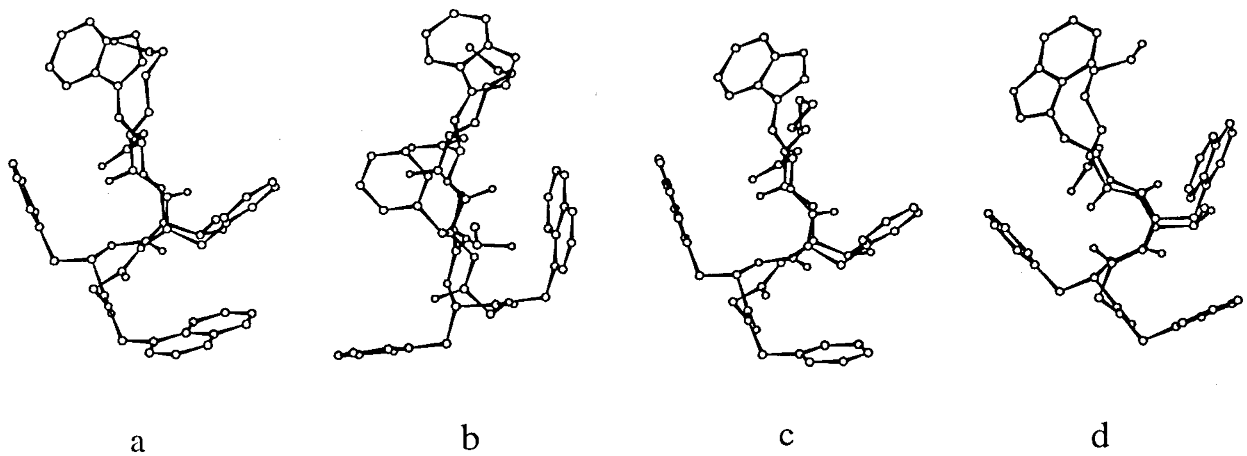

Figure 6 Minimum-energy conformations of the highest populated clusters obtained from free molecular dynamics simulations at 300 K. Structures (**a**) [74 out of 300, lowest energy] and (**b**) [130 out of 300] are those obtained for the **Nnal^{6}** analog. Structure (**c**) [270 out of 300] is obtained for the **Nal^{11}-Nphe^{6}** analog and structure (**d**) [240 out of 300] that obtained for the **Nphe^{6}-Nal^{7}** analog.

the hsst2 receptor, this molecule exhibits the highest hsst5/hsst2 ratio in this series of compounds and has the best selectivity towards the hsst2 receptor.

For the *trans* isomers considerably more flexibility in the type II′ β-turn was found both experimentally and by computer simulations. The high temperature coefficient of the Thr^{10}HN suggests that the type II′ β-turn is very flexible in all three analogs. The instability of the type II′ β-turn which is unambiguously required for bioactivity in the *trans* isomer further supports our assumption that the *cis* and not the *trans* isomers are the bioactive conformations.

Acknowledgements

We wish to thank the National Institutes of Health (DK 15410) for their support of this research. R.M. is grateful for a Deutsche Forschungsgemeinschaft postdoctoral fellowship.

REFERENCES

1. P. Brazeau, W. Vale, R. Burgus, N. Ling, M. Bucher, J. Rivier and R. Guillemin (1973). Hypothalamic polypeptide that inhibits the secretion of the immunoreactive growth hormone. *Science 179*, 77–79.
2. D.J. Koerker, L.A. Harker and C.J. Goodner (1975). Effects of somatostatin on hemostasisin baboons. *Engl. J. Med. 96*, 749–754.
3. J.E. Gerich, R. Lovinger, G.M. Grodsky (1975). Glucagon and insulin release from the perfused rat pancreas in response to arginine, isoproterenol and theophylline: evidence for a preferential effect on glucagon secretion. *Endocrinology 96*, 749–754.
4. D.F. Veber, R.M. Freidinger, D.S. Perlow, W.J. Jr. Palaveda, F.W. Holly, R.G. Strachan, R.F. Nutt, B.J. Arison, C. Homnick, W.C. Randall, M.S. Glitzer, R. Saperstein, R. Hirschmann (1981). R. A potent cyclic hexapeptide analogue of somatostatin. *Nature 292*, 55–58.
5. D.F. Veber. Design and discovery in the development of peptide analogs in: *Peptides, Synthesis, Structure and Function*. Proceedings of the Seventh American Peptide Symposium. D.H. Rich and V.J. Gross, Eds, p. 345–348, Pierce Chemical Co., Rockford, IL, 1983.
6. D.F. Mierke, C. Pattaroni, N. Delaet, A. Toy, M. Goodman, T. Tancredi, A. Motta, P.A. Temussi, L. Moroder, G. Bovermann and E. Wünsch (1990). Cyclic hexapeptides related to somatostatin. *Int. J. Peptide Protein Res. 36*, 418–432.
7. H. Kessler, M. Bernd, H. Kogler, J. Zarbock, O.W. Sorensen; G. Bodenhausen and R.R. Ernst (1983). Peptide conformations. 28. Relayed heteronuclear correlation spectroscopy and conformational analysis of cyclic hexapeptides containing the active sequence of somatostatin. *J. Am. Chem. Soc. 105*, 6944–6952.
8. R.M. Freidinger, D. Perlow Schwenk, W.C. Randall, R. Saperstein, B.H. Arison, D.F. Veber (1984). Conformational modifications of cyclic hexapeptide somatostatin analogs. *Int. J. Peptide Protein Res. 23*, 142–150.
9. D.F. Veber (1982). Peptide analogue design based on conformation. *Spec. Publ. R. Soc. Chem. 42*, 309–319.
10. D.F. Veber, W.C. Randall, R.F. Nutt, R.M. Freidinger, S.F. Brady, D. Perlow Schwenk, P. Curley, R.G. Strachan, F.W. Holly, and R. Saperstein. Circular dichroism aids interpretation of structure-activity relationships of somatostatin analogs, in: *Peptides 1982.*Proceedings of the Seventeenth Europian Peptide Symposium. K. Blaha and P. Malon, Eds, p. 789–792, Walter de Grnyter & Co., Berlin, Germany, 1983.
11. W. Bauer, U. Briner, W. Doepfner, R. Haller, R. Huguenin, P. Merbach, T.J. Petcher and J. Pless (1982). SMS 201-995: A very potent and selective octapeptide analogue of somatostatin with prolonged action. *Life Sci. 31*, 1133–1140.
12. G. Melacini, Q. Zhu, G. Osapay and M. Goodman (1997). A refined model for the somatostatin pharmacophore: conformational analysis of lanthionine-sandostatin analogs. *J. Med. Chem. 40*, 2252–2258.
13. G.M. Smith and D.F. Veber (1986). Computer-aided, systematic search of peptide conformations constrained by NMR data. *Biochem. Biophys. Res. Commun. 134*, 907–923.
14. Z. Huang, Y.-B. He, K. Raynor, M. Tallent and T. Reisine, Goodman (1992). Main chain and side chain chiral methylated somatostatin analogs: Syntheses and conformational analyses. *J. Am. Chem. Soc 114*, 9390–9401.
15. Y.-B. He, Z. Huang, K. Raynor, T. Reisine and M. Goodman (1993). Conformations of somatostatin related cyclic hexapeptides incorporating specific α-methylated and β-methylated residues. *J. Am. Chem. Soc. 115*, 8066–8072.
16. B.H. Arison, R. Hirschmann and D.F. Veber (1978). Bioconformation of somatostatin. *Bioorg. Chem. 7*, 447–451.
17. T.-A. Tran, R.-H. Mattern and M. Goodman. Synthesis and conformational analysis of cyclic hexapeptides related to somatostatin incorporating novel peptoid residues, in: *Proceedings of the American Peptide Symposium*, in press.
18. T.-A. Tran, R.-H. Mattern, M. Afargan, O. Amitay, O. Ziv, B.A. Morgan, J.E. Taylor, D. Hoyer and M. Goodman (1998). Design, synthesis, and biological activities of potent and selective somatostatin analogs incorporating novel peptoid residues. *J. Med. Chem. 41*, 2679–2685.

19. R.-H. Mattern, T.-A. Tran, M. Goodman (1998). Conformational analysis of somatostatin related cyclic hexapeptides containing peptoid residues. *J. Med. Chem. 41*, 2686–2692.
20. T.-A. Tran, R.-H. Mattern, J.E. Taylor, B.A. Morgan and M. Goodman (1999). Synthesis, and binding potencies of cyclohexapeptide somatostatin analogs containing naphthylalanine and arylalkyl peptoid residues. *J. Peptide Sci. 5*, 113–130.
21. D. Davis and A. Bax (1985). Assignment of complex ^{1}H-NMR spectra via two-dimensional homonuclear Hartmann–Hahn spectroscopy. *J. Am. Chem. Soc. 107*, 2820–2821.
22. M.H. Levitt, R. Freeman and T. Frenkiel (1982). Broadband heteronuclear decoupling. *J. Magn. Reson. 47*, 328–330.
23. G. Bodenhausen, R.L. Vold, R.R. Vold (1980). Multiple quantum spin-echo spectroscopy. *J. Magn. Reson. B 37*, 93–106.
24. W.P. Aue, E. Bartholdi and R.R. Ernst (1976). Two-dimensional spectroscopy. Application to nuclear magnetic resonance. *J. Chem. Phys. 64*, 2229–2246.
25. A. Bax and R. Freeman (1981). Investigations of complex networks of spin-spin coupling by two-dimensional NMR. *J. Magn. Reson. 44*, 542–561.
26. M. Rance, O.W. Sorensen, G. Bodenhausen, G. Wagner, R.R. Ernst and K. Wüthrich (1984). Improved spectral resolution in COSY ^{1}H-NMR spectra of proteins via double quantum filters. *Biochem. Biophys. Res. Commun. 117*, 479–485.
27. A.A. Bothner-By, R.L. Stephens, J. Lee, C.D. Warren and R.W. Jeanloz (1984). Structure determination of a tetrasaccharide: transient nuclear Overhauser effects in the rotating frame. *J. Am. Chem. Soc. 106*, 811–813.
28. K. Wüthrich, in: *NMR of Proteins and Nucleic Acids*. Wiley, New York, 1986.
29. V.F. Bystrov, V.T. Ivanov, S.L. Portanova, T.A. Balashova and Y.A. Ovchinnikov (1973). Refinement of the angular dependence of the peptide vicinal NH-Ca$^{\alpha}$H coupling constant. *Tetrahedron 29*, 873–877.
30. M.T. Cung, M. Marraud and J. Néel (1974). Experimental calibration of a Karplus relationship in order to study the conformations of peptides by nuclear magnetic resonance. *Macromolecules 7*, 606–613.
31. K.G.P. Pachler (1964). Nuclear magnetic resonance study of some α-amino acids—II. Rotational isomerism. *Spectrochim. Acta 20*, 581–587.
32. M.T. Cung and M. Marraud (1982). Conformational dependence of the vicinal proton coupling constant for the C$^{\alpha}$-C$^{\beta}$ bond in peptides. *Biopolymers 21*, 953–967.
33. T. Yamazaki, A. Probstl, P.W. Schiller and M. Goodman (1991). Biological and conformational studies of [Val^4]morphiceptin and [D-Val^4]morphiceptin analogs incorporating *cis*-2-aminocyclopentane carboxylic acids as peptidomimetic for proline. *Int. J. Peptide Protein Res. 37*, 364–381.
34. J.M. Blaney, G.M. Crippen, A. Dearing, J.S. Dixon, J.S., E.I. du Pont de Nemours and Company Experimental Station. *DGEOM*, *Quantum Chemistry Program Exchange Program No. 590*, Wilmington, DE 19898.
35. Discover 95.0/3.00 User Guide, Biosym/MSI, San Diego, CA, 1995.

